Eur. Phys. J. D **44**, 337–344 (2007)
DOI: 10.1140/epjd/e2007-00180-y

THE EUROPEAN PHYSICAL JOURNAL D

Molecular-beam scattering and pressure broadening cross sections for the acetylene-neon system

F. Thibault[1,a], D. Cappelletti[2], F. Pirani[3], G. Blanquet[4], and M. Bartolomei[5]

[1] Laboratoire de Physique des Atomes Lasers Molécules et Surfaces (UMR-CNRS 6627), Université de Rennes I, Campus de Beaulieu, 35042 Rennes Cedex, France
[2] Dipartimento di Ingegneria Civile ed Ambientale, Universita' di Perugia, Perugia, Italy
[3] Dipartimento di Chimica, Universita' di Perugia, Perugia, Italy
[4] Laboratoire de Spectroscopie Moléculaire, Facultés Universitaires Notre-Dame de la Paix, 5000 Namur, Belgium
[5] Instituto de Matemáticas y Física Fundamental, CSIC, c/ Serrano 123, 28006 Madrid, Spain

Received 21 March 2007
Published online 1st June 2007 –

Abstract. Integral cross sections and pressure broadening coefficients have been measured for the acetylene — neon system by a molecular beam scattering technique and by high infrared resolution spectroscopy, respectively. We have performed quantal calculations using an ab-initio potential energy surface (PES) [J. Chem. Phys. **109**, 8968 (1998)]. Results are found to be in good agreement with both measured integral cross sections and pressure broadening coefficients for the two temperatures investigated (173 and 298 K). We have also derived a semi-empirical PES parameterized using an atom-bond pairwise additive scheme. This PES shows an isotropic component in agreement with the ab-initio calculation, reproduces the scattering data but it only leads to a reasonable agreement for the pressure broadening coefficients.

PACS. 31.50.-x Potential energy surfaces – 33.15.Bh General molecular conformation and symmetry; stereochemistry – 33.20.Ea Infrared spectra – 33.70.-w Intensities and shapes of molecular spectral lines and bands

1 Introduction

Acetylene is a trace constituent of the Earth's atmosphere mainly produced by anthropogenic sources [1] and is essentially destroyed by chemical reactions with Cl^- and OH^-. The study of this molecule provides valuable information for the understanding of the ozone cycle as well as for the development of pollution transport models. Acetylene has also been detected in the atmosphere of giant planets (Jupiter, Saturn, Uranus and Neptune) [2,3], and Titan [4]. Photolysis of methane by solar radiation yields various product hydrocarbons of which the most abundant are ethane and acetylene [5]. In 2004, Mars Express confirmed the presence of methane in the Martian atmosphere where various rare gases are also present. Moreover, acetylene is involved in many processes relevant to combustion and the simplicity of its spectra is well suited for thermometry applications using vibrational or rotational coherent anti-Stokes Raman scattering (CARS) (see Ref. [6] and references therein).

For all the above applications, a detailed knowledge of collisional line broadening is required. Many experimental and theoretical studies have been devoted to both IR and Raman spectra of acetylene diluted in atomic or molecular mixtures [6–9]. To our knowledge only two (experimental) works dealt with neon [10,11]. Moreover, the measure of pressure broadening coefficients may be useful to test the accuracy of a potential energy surface (PES) especially if experimental values are available over a wide range of temperatures [8,9,12].

Weakly bound complexes involving acetylene interacting with rare gas atoms have received much attention in recent years, because of their peculiar intermolecular potential mainly affected by the interaction of the rare gas atom with the triple bond of acetylene. The interactions of acetylene with helium and the heavier rare gas atoms have been thoroughly investigated [8,12–17].

For the present case, the Ne-C_2H_2 complex, Bemish et al. [15] carried out a complementary experimental and theoretical characterization. They constructed the first ab-initio PES for this system by using the SAPT method. This SAPT PES was employed to interpret the infrared spectra (in the ν_3 band region of the monomer) of the Ne-C_2H_2 and Ne-C_2HD complexes, measured by the same authors [15]. The measured [16] microwave spectrum has also been used to test this PES. A more recent ab-initio calculation [17] with the CCSD(T) methodology has substantially confirmed the value of the energy for the absolute

[a] e-mail: franck.thibault@univ-rennes1.fr

minimum but suggesting an appreciably larger (4%) equilibrium distance.

Herein, we present a further experimental investigation of this system, based on measurements of integral scattering cross sections (ICS) and pressure broadening (PB) coefficients. These data, which provide information complementary to spectroscopy, are used to test the accuracy of the available SAPT PES by comparisons with dynamical calculations.

Due to the difficulties of determining full ab-initio PESs, semi-empirical methods, which rely upon available experimental data, are often used in their determination. This approach is successful as demonstrated by many authors and recently pursued by us for the cases of Ar-C_2H_2 [8,12] and Kr-, Xe-C_2H_2 [12]. In order to complete this study an empirical model PES has also been generated for Ne-C_2H_2 by using the atom-bond pairwise additive method developed in Perugia [18–20]. One of the objectives of these studies is to characterize C-C and C-H interactions with rare gases using simple parameterization and simple potential expression for more complex systems [18–22].

Our paper is organized as follows. Section 2 describes the experimental set up for the scattering and pressure broadening measurements. In Section 3 we will illustrate the features of the SAPT and atom-bond PESs utilized in this work. Comparison of calculations using these two PESs with the experimental data will be carried out in Section 4. Finally, discussions and concluding remarks are presented in Section 5.

2 Experiments

2.1 Integral cross sections

The experimental apparatus has been already described in detail previously [21] and almost all of the experimental detail are similar to those already reported for the study of the acetylene-Ar complex [8], so that they will not be reported in this paper. The total (elastic + inelastic) ICS Q is obtained at a given selected molecular beam velocity v by measuring the molecular beam intensity attenuation due to the presence of the target gas in the scattering box. The calibration of the absolute scale of $Q(v)$ is obtained following the procedure illustrated in reference [23]. The apparatus operates under high angular and velocity resolution conditions, which are necessary in order to measure "glory" quantum interference effects in $Q(v)$.

Experimental results are shown in Figure 1, where $Q(v)$ is plotted multiplied by the factor $v^{2/5}$ as usual to separate the "glory" pattern from the behaviour of the average component of the cross sections. It is important to note that in the present experimental conditions the inelastic contribution to $Q(v)$ is expected to be negligible with respect to the elastic one. Indeed, for the investigated system we resolved "glory" structures clearly, not "quenched" by inelastic effects. Therefore, in the observed glory region $Q(v)$ is influenced mainly by collisions at intermediate and large impact parameters, where the probability of inelastic events is scarce [24]. In the present experimental conditions the molecular beam essentially contains "rotationally hot" acetylene molecules.

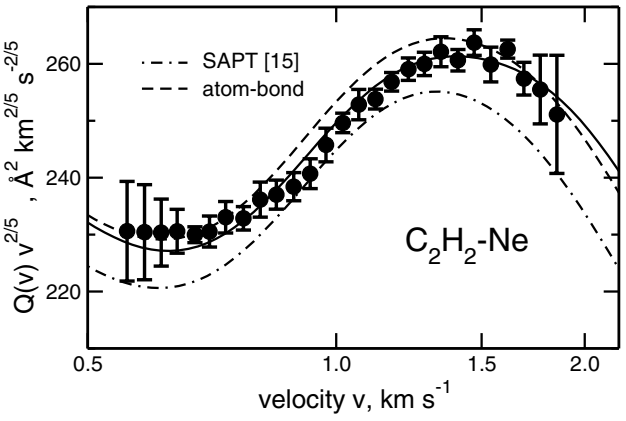

Fig. 1. Experimental total cross sections $Q(v)$ for scattering of a rotationally "hot" and nearly effusive acetylene molecular beam by neon targets. Data are plotted as $Q(v) \times v^{2/5}$ (see text), as a function of the beam velocity v. Dot-dashed line are calculations with the SAPT PES, dashed line with parameters provided in Table 2, continuous line best fit: see Section 4.1.

"Hot" conditions refer to the comparison between the average rotational energy of molecules and the collision energy explored in the scattering process. An evaluation of these parameters based on the probed v range and on the temperature of the heated molecular beam source suggests that a neon atom, during a collision with a C_2H_2 molecule, at the moderate and low v of the present experiment, essentially feels an isotropic force field. This is because the C_2H_2 molecule rotates sufficiently fast to average the interaction potential anisotropy. In these conditions C_2H_2 tends to behave like a pseudo-atom, so that an effective radial potential very similar to the spherical average of the PES is expected to govern the collision.

2.2 Pressure broadening coefficients

The spectra were recorded with an improved Laser Analytics (LS3 model) tunable diode-laser spectrometer described in detail elsewhere [25]. The gas samples were provided by l'Air Liquide, acetylene with a stated purity of 99.6% and neon with a stated purity of 99.99%. For the measurements at room temperature, the absorption cell was a White type multipass cell with 1 meter between mirrors. The chosen path length was 8.17 m; the partial pressure of C_2H_2 was ranging between 0.01 and 0.10 mbar and the pressure of Ne varied from 35 to 65 mbar. At low temperatures (173 K) we used a single pass cell described in detail in reference [26]. The optical path length was 40.43 cm and the temperature of the gas kept constant to ± 0.5 K. In this case, the partial pressure of C_2H_2 was ranging between 0.04 and 0.32 mbar and the pressure of Ne between 35 and 70 mbar. For each line under study we used four different pressures of Ne, the partial pressure of C_2H_2 was constant in the mixtures. The pressures were

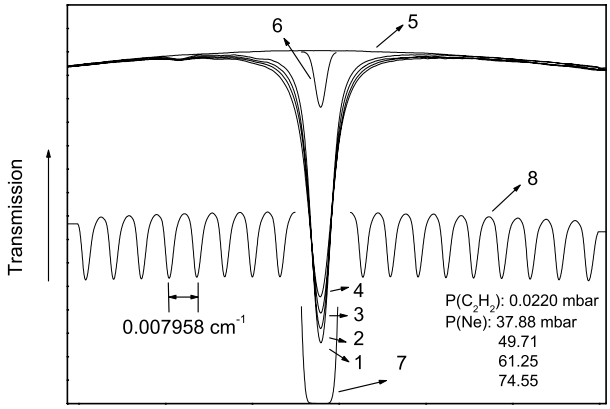

Fig. 2. Example of the spectra obtained for the $R(16)$ line in the $\nu_4+\nu_5$ band of C_2H_2 perturbed by Ne at room temperature: (1–4) broadened line at 37.88, 49.71, 61.25, and 74.55 mbar of Ne; (5) diode-laser emission profile recorded with an empty cell; (6) low pressure C_2H_2 line (Doppler regime); (7) saturated line; (8) confocal étalon fringes.

measured at room temperature with two MKS baratron gauges with a full scale reading of 1.2 and 120 mbar. The relative spectral calibration was obtained by introducing in the laser beam a confocal étalon with a free spectral interval of 0.007958 cm^{-1}. The assignments and wavenumbers of the measured lines of C_2H_2 in the $\nu_4+\nu_5$ band are taken from reference [27].

Eight consecutive spectra are necessary in order to study one line: the record of the empty cell which represents the laser emission profile, the four broadened lines at different neon pressures with a constant C_2H_2 pressure, the étalon fringes with the cell evacuated, the pure C_2H_2 line at very low pressure ($\leq$0.01 mbar) providing an effective Doppler profile used to evaluate the apparatus function, and a saturated spectrum of this line giving the 0% transmission level. An example of the spectra obtained for the line $R(16)$ of C_2H_2 at 1369.0519 cm^{-1} is shown in Figure 2. After being recorded, the spectra were linearized in frequency to correct the slightly nonlinear tuning of the diode-laser with a constant step of about 1×10^{-4} cm^{-1}.

The measurements have been performed on 10 lines distributed in the P and R branches between $P(2)$ and $R(26)$ at room temperature and 9 lines at low temperature (173 K) at the same j except $R(26)$.

2.3 Data reduction and experimental results of the pressure broadening coefficients

The procedure used for data reduction is similar to the method described in detail in reference [28]. To obtain the collisional halfwidths γ_c at half maximum, we have fitted the Voigt and the Rautian profiles on the measured absorbance $\alpha(\nu)$ defined by the Beer-Lambert law (see Eq. (1) of Ref. [28]). In the fitting procedure, the Doppler width was fixed and three or four parameters are respectively determined by a non-linear subroutine. These parameters are: the line position ν_c; the collisional halfwidth γ_c, an intensity factor and for the Rautian model, the narrowing parameter β_c which is associated with velocity effects on the spectral line shape (see references therein [28]). Small instrumental distortions were taken into account by using an effective Doppler halfwidth γ_D instead of the true Doppler halfwidth γ_{Dth} ($\gamma_D = \sqrt{\gamma_{Dth}^2 + \gamma_{app}^2}$). The apparatus function may be assimilated to a Gaussian function with a halfwidth γ_{app} which had a typical value of about 5×10^{-4} cm^{-1}.

The normalized, per neon atmosphere, broadening coefficients γ_0 are obtained by least squares fitting of the pressure dependence of the collisional halfwidth γ_c. The results are presented in Table 1 for the two considered temperatures (297 K and 173 K). The given error is twice the standard deviation plus 2% of γ_0 to take into account various errors: the baseline location, the perturbation due to nearby interfering lines, the nonlinear tuning of the laser and the approximate lineshape model used.

3 Potential energy surfaces

The present experimental results were used to test two potential energy surfaces for the Ne-C_2H_2 complex. The first PES has been provided by the SAPT calculations of Bemish et al. [15] whose detail have been discussed in the original paper by the authors. The second PES is of the atom-bond type [18]. Detail of the parameterization can be found in [8,18]. Essentially, the interaction energy is represented here as sum of 3 atom-bond contributions:

$$V_{ab}(r,\alpha) = \varepsilon(\alpha)\left[\frac{6}{n(r,\alpha)-6}\left(\frac{r_m(\alpha)}{r}\right)^{n(r,\alpha)} - \frac{n(r,\alpha)}{n(r,\alpha)-6}\left(\frac{r_m(\alpha)}{r}\right)^6\right] \quad (1)$$

with

$$n(r,\alpha) = 9 + 4\left(\frac{r}{r_m(\alpha)}\right)^2. \quad (2)$$

r is the distance of the neon atom from the bond center and α is the angle that $\boldsymbol{r}$ forms with the bond axis considered. The dependence of the potential well depth and its location is given by the following relationships:

$$\varepsilon(\alpha) = \varepsilon_\perp \sin^2(\alpha) + \varepsilon_\parallel \cos^2(\alpha) \quad (3)$$

$$r_m(\alpha) = r_{m\perp} \sin^2(\alpha) + r_{m\parallel} \cos^2(\alpha) \quad (4)$$

where $\varepsilon_{m\perp,\parallel}$, $r_{m\perp,\parallel}$ are these equilibrium parameters for respectively the perpendicular and parallel approaches of the rare gas atom to the bond.

The Ne-CH bond pair parameters were fixed to the values obtained in the past for CH_4-Ne [19], C_2H_4-Ne [22] and C_6H_6-Ne [21] PESs. The ones of the Ne-CC triple bond pair were obtained by an empirical scaling [20] of those of the C_2H_2-Ar case [8,12]. We have optimized these parameters in order to better reproduce the measured pressure

Table 1. Pressure broadening coefficients and their temperature dependence. * Experimental HWHM for P lines, all other values for R lines; profile adjusted with (a) a Voigt profile and (b) a Rautian profile.

Line	$T = 298$ K			$T = 173$ K			n
M	VP(a)	RP(b)	CC/CS	VP(a)	RP(b)	CC/CS	
1*	50.6(1.2)	52.3(1.6)	48.9	74.7(2.4)	76.6(2.3)	74.5	0.79
2*	46.1(1.3)	47.6(1.3)	46.25	68.1(2.5)	69.2(2.2)	67.8	0.68
3			43.95			64.	0.67
4			42.05			60.7	0.65
5	41.5(1.1)	43.5(1.1)	40.40	58.5(1.7)	59.4(1.7)	57.85	0.64
6			38.95			55.15	0.62
7	38.2(1.1)	40.3(1.1)	38.00	52.9(1.7)	54.9(1.5)	53.75	0.61
8			37.40			52.9	0.61
9			37.15			52.85	0.62
10	36.8(0.8)	37.8(1.2)	36.90	51.5(1.3)	52.7(1.6)	52.6	0.62
11			36.40			51.8	0.61
12	37.5(0.9	39.3(1.)	36.40	52.1(1.5)	55.4(1.8)	51.7	0.61
13			36.25			51.2	0.60
14			36.05			50.5	0.59
15	33.8(1.2)	36.4(0.9)	35.80	47.8(1.8)	50.2(1.3)	49.65	0.58
16			35.40			48.55	0.57
17	33.1(0.9)	35.7(1.2)	34.90	44.7(1.9)	48.0(1.2)	47.4	0.55
18			34.50			46.25	0.54
19			33.75			44.9	0.52
20			33.10			43.55	0.50
21			32.30			42.25	0.50
22	30.1(0.8)	33.0(1.)		38.5(1.4)	41.4(1.5)		
27	25.3(0.8)	29.4(1.)					

Table 2. Interaction potential parameters for the C_2H_2-Ne system, see equations (1–4), distances are in Bohr and energies in meV (1 meV = 8.06554 cm^{-1}).

pair	$r_{m\perp}$	$r_{m\parallel}$	$\varepsilon_{m\perp}$	$\varepsilon_{m\parallel}$
C≡C + Ne	7.237	7.615	3.48	4.12
C–H + Ne	6.266	6.707	2.544	1.96

broadening coefficients (see below). The final values are reported in Table 2.

A comparison between the SAPT and atom-bond PESs is shown in Figure 3 where some angular cuts in the intermolecular range of interest for our experiments are displayed. These cuts are overall quite similar. In general the semi-empirical PES is more repulsive than the SAPT one at short range for all fixed angular orientations. The absolute minimum of the present PES is found for a bent geometry of about 60 degrees while for the SAPT PES it is found at about 45 degrees.

The PESs were then projected in Legendre polynomials:

$$V(R,\theta) = \sum_{\lambda=0}^{10} V_\lambda(R) P_\lambda(\cos\theta) \qquad (5)$$

with the help of a 16-point Gauss-Legendre quadrature (note that only half of these points are really necessary because of the symmetry of the PES). R is the distance from the center of this linear molecule and the neon atom and θ is the angle between R and the molecular axis. The

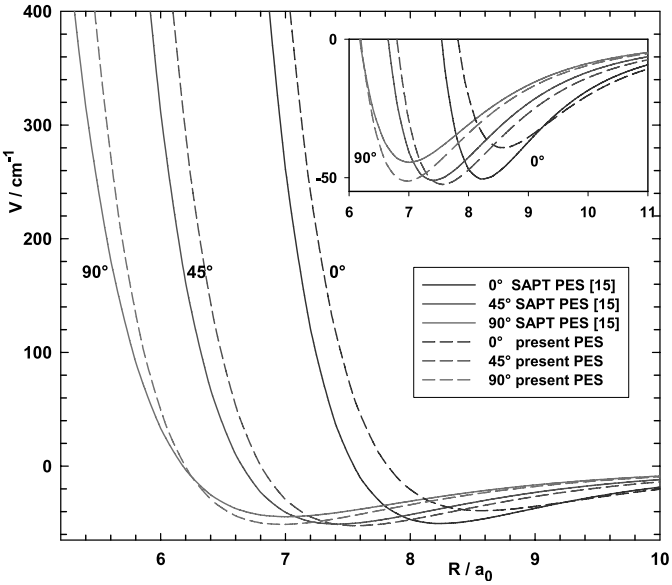

Fig. 3. Comparison between the present (dashed lines) and SAPT [15] (solid lines) PESs for selected fixed orientations.

V_0, V_2, V_4 terms are shown to further compare with the ab-initio results in Figure 4. As can be appreciated from the figure the leading V_0 term, which accounts essentially for the spherical average interaction, is very similar for the two cases.

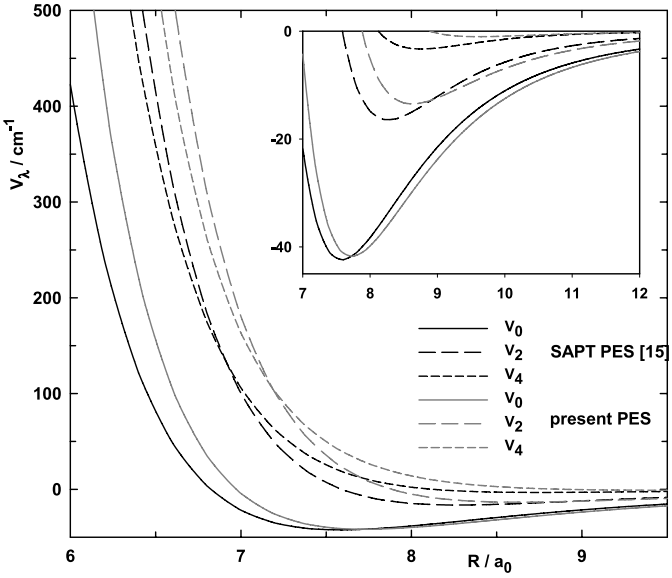

Fig. 4. Comparison between the present and SAPT [15] isotropic and main anisotropic terms.

4 Comparisons of scattering and pressure broadening cross sections with calculations

4.1 Integral cross sections

Scattering cross sections are described using a dynamical model developed for collisions of light hydrocarbons and recently applied to study C_2H_4 [22] and C_2H_2 [8,12] collisions. Briefly, the dynamics are described as falling into two different limiting regimes. A pseudo-atom regime is assumed at low collision energies, dominated by an isotropic force field. A molecular regime sets in at higher collision velocities. The dynamics are modeled according to both low and high helicity decoupling schemes (see Refs. [8,12,22] for detail). The final calculated ICS have been obtained within the spherical model for $v < 0.9$ km s^{-1} and in accordance to the molecular model for $v > 1.9$ km s^{-1}. The switch between the two dynamical regimes at intermediate velocities has been carried out by a weighted sum (the weights depending on the velocity) of cross sections calculated for the two limiting cases. The scattering cross sections have been calculated in the center of mass system. Standard numerical techniques have been used for the phase shift evaluation [29]. The cross sections have been then convoluted in the laboratory frame and are compared with the experimental data in Figure 1 for both the SAPT and the atom-bond PESs.

The results for the SAPT PES (Fig. 1) are in satisfactory agreement with the experiments: the glory extremum position is well reproduced and there is only a minor deviation (about 2%) on the absolute value of the cross sections, which is at the limit of the experimental uncertainty, and indicates a slight underestimation of the overall attraction at long range. The overall agreement is a demonstration that the spherical average interaction of the SAPT PES is accurate and reliable in an absolute scale, for intermediate and large intermolecular distances.

For the atom-bond PES two sets of calculations are shown in Figure 1. The continuous line corresponds to potential parameters of the Ne-CC triple bond pair as obtained by the direct scaling of the Ar-acetylene ones. The dashed curve has been calculated with slightly different Ne-CC triple bond pair parameters, adjusted in order to better reproduce also the pressure broadening coefficients. As it can be seen the latter gave a less good agreement with the scattering cross sections, at the limit of the experimental uncertainty. These parameters are those reported in Table 2 as final best fit parameters.

4.2 Pressure broadening cross sections

Pressure broadening cross sections have been derived [30,31] from binary scattering S-matrix elements computed by MOLSCAT [32] quantum dynamical code and its parallelized version by McBane [33]. Therefore, the impact approximation is assumed [30,34,35]. The coupled equations were solved by means of the hybrid log derivative — Airy propagator of Alexander and Manolopoulos [36]. The propagation is carried out with the diabatic modified log-derivative method from a minimum distance of 2 Å to an intermediate one of 15 Å and with the Airy method up to a maximum intermolecular distance $R = 30$ Å. For the $R(j = 0)$ line, convergence in the cross sections is typically reached for total angular momentum J of about 60 and 80 for kinetic energies of 153 cm^{-1} and 263 cm^{-1} respectively. As the rotational quantum number j increases less J values are needed [37], because associated pressure broadening cross sections are less sensitive to large impact parameters. Here $\boldsymbol{J} = \boldsymbol{j} + \boldsymbol{\ell}$, in which ℓ is associated with the relative motion of the colliding pair.

In order to economize CPU time, the radial coefficients $V_\lambda(R)$ (Eq. (5) for R ranging from 1 to 15 Å were precomputed and stored in a file and then used in (subsequent) MOLSCAT runs in conjunction with standard interpolation and extrapolations routines. Note that in the domain of energies we investigated our calculations are not sensitive to these extrapolations (of C_x/R^x form at long range).

All energetically open rotational levels and at least four closed levels, two with odd and two with even rotational angular j, are included in the calculations for each total energy $E_T = E_{kin} + E_{Rot}(j)$. Since we compare our calculations with experimental PB coefficients for P or R lines we had to consider both species (ortho and para) of acetylene simultaneously. The rotational energy levels were generated with a fixed rotational constant ($B = 1.176641$ cm^{-1}) and the same PES was considered in both ground and vibrationally excited states of C_2H_2. Indeed, the different PESs considered here do not include any vibrational dependence. In the rigid rotor approximation we assume the collisional width for a $R(j)$ line to be equal to the width of the $P(j + 1)$ line [30].

The collisional halfwidth at half maximum (HWHM), associated with a sample at temperature T, is obtained by assuming a Maxwellian thermal distribution of the colliding particles:

$$\gamma(j;T) = n_b \langle v \sigma_{PB}(j;E_{kin}) \rangle \equiv n_b \bar{v} \bar{\sigma}_{PB}(j;T) \qquad (6)$$

$$\bar{\sigma}_{PB}(j;T) = \left(\frac{1}{k_B T}\right)^2 \int_0^\infty E_{kin}\sigma_{PB}(j;E_{kin}) \times \exp(-E_{kin}/k_B T)dE_{kin} \quad (7)$$

where n_b is the density of the perturbers, $\bar{v} = \sqrt{8k_BT/(\pi\mu)}$ is the mean relative velocity for a sample at temperature T and σ_{PB} stands for the real part of the generalized [30] cross section $\sigma^{(1)}$ since we deal with IR lines. Therefore, the normalized (in cm^{-1} atm^{-1}) collisional HWHM may be written as:

$$\gamma_o = \frac{\bar{v}\bar{\sigma}_{PB}}{2\pi c k_B T} = 56.6915(\mu T)^{-1/2}\bar{\sigma}_{PB} \times 10^{-3} \quad (8)$$

in which μ is the radiator — perturber reduced mass ($\mu_{C_2H_2-Ne}$= 11.31 a.m.u.) and the cross section is in Å^2.

For the SAPT PES, in order to perform the thermal average the close coupling (CC) method [38] was used to compute pressure broadening cross sections, for all the investigated lines, over 17 kinetic energies between 5 and 360 cm^{-1}. The less accurate, but less time consuming, coupled states (CS) method [39–41] was used for 6 higher kinetic energies between 420 and 2000 cm^{-1}. Note that the weight of the latter data in the thermal average is small at our temperatures, such that the accuracy of our results is essentially determined by the precision of the close coupling method. Moreover, as expected, because of its impulsive character the CS approximation works better as the kinetic energy and j increase because in these cases the collision dynamic is mainly governed by the repulsive part of the PES [7,37,42–45].

Pressure broadening cross sections calculated at the mean kinetic energies of 153 cm^{-1} and 263 cm^{-1} ($\bar{E}_{kin} = 4k_BT/\pi$ in cm^{-1} for T = 173 and 297 K resp.) are quite in good agreement with thermally averaged pressure broadening cross sections at the corresponding temperatures. Figure 5 provides a comparison between thermally averaged HWHM and unaveraged values obtained from cross sections calculated at $\bar{E}_{kin}$ (in Eq. (8) $\bar{\sigma}_{PB}$ is replaced by $\sigma_{PB}(\bar{E}_{kin})$ still using the SAPT PES. The two types of calculations tend to converge as the temperature increases because the pressure broadening cross sections becomes a slowly varying function of the kinetic energy. At 173 K the maximum relative difference is 6.6% for the $R(9)$ line and at 297 K the maximum relative error is 3.3% for the $R(12)$ line. This observation, already noticed in references [42–44] for other optically active molecules and in references [7–9,12] for the Rg-C_2H_2 systems, led us to perform CC calculations with the present semi-empirical PES at the single kinetic energies $\bar{E}_{kin}$= 153 and 263 cm^{-1} only.

The agreement of the CC/CS thermally averaged pressure broadening coefficients, obtained with the SAPT PES, with the experimental values is very satisfactory while the unaveraged values are only in fair agreement with the measured values (Fig. 5). The good agreement found with our rigid rotor model confirms the absence of significant vibrational effects [8,10–12]. Moreover, our measurements were carried out in the $\nu_4+\nu_5$ combination

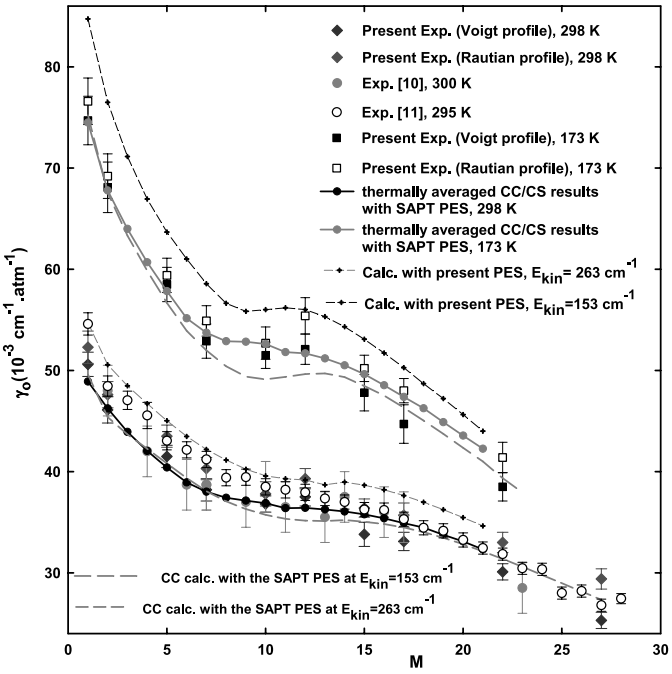

Fig. 5. Comparison between various calculations of PB coefficients performed with the present atom-bond and the SAPT [15] PESs with experimental values of references [10,11] and present experimental values at 173 and 298 K.

vibrational band while those of Valipour et al. [10] were performed in the $\nu_1+3\nu_3$ combination overtone band and those of Hardwick et al. [11] in the $\nu_1+\nu_3$ band.

The values calculated using the present semi-empirical PES fall at the upper limit of the experimental data. We consider this comparison less good than for the SAPT PES even if still reasonable (Fig. 5). This can be explained by writing, from semi-classical arguments $\sigma_{PB} \approx \pi b^2$, where b is an effective scaling length. From this formula we can estimate that, between 173 and 298 K, our calculations probe the PES roughly between 6.15 and 8.15 Bohr. In this region the atom-bond PES is more repulsive and more anisotropic than the SAPT PES (see Figs. 3, 4), thus leading to more rotational exchanges and consequently to larger PB cross sections.

As an additional result we have calculated, with the SAPT PES, pressure broadening coefficients at various temperatures between 77 and 1000 K. Of course, for T greater than 400 K these are mainly CS values. This permits us to obtain the temperature dependence of the HWHM using:

$$\gamma_0(T) = \gamma_0(T_0)\left(\frac{T_0}{T}\right)^n \quad (9)$$

with T_0 = 298 K. This simple power law may be safely used between ∼173 and 1000 K and Table 1 provides an averaged $\bar{n}$ exponent. This may be useful in an experiment as a first guess of the linewidths. As expected, for the highest js $\bar{n}$ tends to its classical limit (0.5), especially when T increases. For more accurate values, calculated HWHM at various temperatures are available on request.

5 Conclusions

We have presented new experimental results and calculations useful for characterizing the structure and potential energy of the acetylene-neon system. In particular integral scattering cross section as a function of collision energy and pressure broadening coefficients, at temperatures $T = 298$ and 173 K, have been measured. Quantal calculations performed on the SAPT PES of reference [15] provide very good overall agreement with all the experimental data indicating that both the spherical and the anisotropic components of the interaction are very accurate.

We have also generated a semi-empirical PES of the atom-bond type [19] by scaling, with empirical correlation formulas [20], the parameters of the analogous acetylene-Ar system [8]. Comparison with experimental data suggests that the average component of the atom-bond PES is very accurate while its anisotropy is realistic but not as accurate as that of the SAPT PES. In general the results obtained here and in references [8,12] pursuing the method developed in Perugia and using predetermined parameters characterizing the interactions [18,19,21,22] are encouraging. The overall behaviour of the integral and pressure broadening cross sections of acetylene interacting with Ne, Ar, Kr and Xe is correct. The simple form of the PESs expressed with the help of a few parameters may be used as a starting material for studying more complex hydrocarbons interacting with these rare gases.

This work ends a series of papers devoted to rare-gas broadened C_2H_2 lines. The overall trend of our theoretical pressure broadening cross sections is supported by recent measurements performed at room temperature at the University of Oregon [11] with these perturbers, this confirms the accuracy of the present values and of those previously reported in references [8,9,12]. Next challenge will be the study of the interaction between acetylene and diatomic molecules. This work is in progress.

The work in Perugia has been supported by the Italian Ministero della Universitá e Ricerca (MIUR) through PRIN 2005 contract No. 2005033911_001. M.B. was supported by the "Juan de la Cierva" programme of the Ministerio de Educación y Ciencia. We would also like to thank John Hardwick for making his results available to us prior publication and Robert Moszynski for having provided the code to generate the SAPT C_2H_2-Ne PES.

References

1. A. Goldman, F.J. Murcray, R.D. Blatherwhick, J.R. Gillis, F.S. Bonomo, F.H. Murcray, D.G. Murcray, J. Geophys. Res. **86**, 12143 (1981)
2. Th. Encrenaz, P. Drossart, H. Feuchtgruber, E. Lellouch, B. Bézard, T. Fouchet, S.K. Atreya, Planet. Space Sci. **47**, 1225 (1999)
3. P.V. Sada, G.L. Bjoraker, D.E. Jennings, P.N. Romani, G.H. McCabe, Icarus **173**, 499 (2005)
4. R. Lorenz , J. Phys. IV France **12**, 281 (2002)
5. R. Hanel, B. Conrath, M. Flasar, V.G. Kunde, W. Maguire, J. Pearl, J. Pirraglia, R.C. Samuelson, L. Herath, L. Allison, D. Cruickshank, D. Gauthier, P. Gierasch, L. Horn, S. Kumar, C. Ponnamperuma, Science **212**, 192 (1981)
6. J. Buldyreva, J. Bonamy, M.C. Weikl, F. Beyrau, T. Seeger, A. Leipertz, F. Vestin, M. Afzelius, J. Bood, P.-E. Bengtsson, J. Raman Spectrosc. **37**, 647 (2006)
7. J.L. Domenech, F. Thibault, D. Bermejo, J.-P. Bouanich, J. Mol. Spectrosc. **225**, 48 (2004)
8. D. Cappelletti, M. Bartolomei, M. Sabido, F. Pirani, G. Blanquet, J. Walrand, J.-P. Bouanich, F. Thibault, J. Phys. Chem. A **109**, 8471 (2005)
9. F. Thibault, J. Mol. Spectrosc. **234**, 286 (2005)
10. H. Valipour, D. Zimmermann, J. Chem. Phys. **114**, 3535 (2001)
11. J.L. Hardwick, S.W. Arteaga, C.M. Bejger, J.L. Gerecke, Z.T. Martin, J. Mayo, E.A. McIlhattan, J.-M.F. Moreau, M.J. Pilkenton, M.J. Polston, B.T. Robertson, E.N. Wolf, J. Mol. Spectrosc. (to be published)
12. D. Cappelletti, M. Bartolomei, E. Carmona-Novillo, F. Pirani, G. Blanquet, F. Thibault, J. Chem. Phys. **126**, 064311 (2007)
13. M. Yang, R.O. Watts, J. Chem. Phys. **105**, 3582 (1994)
14. R. Moszynski, P.E.S. Wormer, A. van der Avoird, J. Chem. Phys. **102**, 8385 (1995)
15. R.J. Bemish, L. Oudejans, R.E. Miller, R. Moszynski, T.G.A. Heijmen, T. Korona, P.E.S. Wormer, A. van der Avoird, J. Chem. Phys. **109**, 8968 (1998)
16. Y. Liu, W. Jäger, Phys. Chem. Chem. Phys. **5**, 1744 (2003)
17. C.R. Munteanu, B. Fernández, J. Chem. Phys. **123**, 014309 (2005)
18. F. Pirani, D. Cappelletti, G. Liuti, Chem. Phys. Lett. **350**, 286 (2001)
19. F. Pirani, M. Albertì, A. Castro, M. Moix Teixidor, D. Cappelletti, Chem. Phys. Lett. **394**, 37 (2004)
20. R. Cambi, D. Cappelletti, F. Pirani, G. Liuti, J. Chem. Phys. **95**, 1852 (1991)
21. D. Cappelletti, M. Bartolomei, V. Aquilanti, F. Pirani, J. Phys. Chem. A **106**, 10764 (2002)
22. D. Cappelletti, M. Bartolomei, V. Aquilanti, F. Pirani, Chem. Phys. Lett. **420**, 100 (2006)
23. V. Aquilanti, D. Ascenzi, M. Bartolomei, D. Cappelletti, S. Cavalli, M. DeCastro Vitores, F. Pirani, J. Am. Chem. Soc. **121**, 10794 (1999)
24. V. Aquilanti, D. Ascenzi, D. Cappelletti, M. De Castro, F. Pirani, J. Chem. Phys. **109**, 3898 (1998)
25. M. Lepère, G. Blanquet, J. Walrand, J.-P. Bouanich, J. Mol. Spectrosc. **181**, 345 (1997)
26. Ch. Lerot, J. Walrand, G. Blanquet, J.-P. Bouanich, M. Lepère, J. Mol. Spectrosc. **219**, 329 (2003)
27. Y. Kabbadj, M. Herman, G. Di Lonardo, L. Fusina, J.W.C. Johns, J. Mol. Spectrosc. **150**, 535 (1991)
28. J.-P. Bouanich, G. Blanquet, J. Walrand, J. Mol. Spectrosc. **219**, 98 (2003)
29. F. Pirani, F. Vecchiocattivi, Mol. Phys. **45**, 1003 (1982)
30. A. Ben-Reuven, Phys. Rev. **141**, 34 (1966);
    A. Ben-Reuven, Phys. Rev. **145**, 7 (1966)
31. R. Shafer, R.G. Gordon, J. Chem. Phys. **58**, 5422 (1973)
32. J.M. Hutson, S. Green, MOLSCAT version 14, Collaborative Computational Project 6 of the UK Science and Engineering Research Council, Daresbury Laboratory, UK (1995)

33. George C. McBane, "PMP Molscat", a parallel version of Molscat version 14 available at `http://faculty.gvsu.edu/mcbaneg/pmpmolscat`, Grand Valley State University (2005)
34. M. Baranger, Phys. Rev. **111**, 481 (1958); M. Baranger, Phys. Rev. **111**, 494 (1958); M. Baranger, Phys. Rev. **112**, 855 (1958)
35. U. Fano, Phys. Rev. **131**, 259 (1963)
36. M.H. Alexander, D.E. Manolopoulos, J. Chem. Phys. **86**, 2044 (1987)
37. C.F. Roche, A.S. Dickinson, J.M. Hutson, J. Chem. Phys. **111**, 5824 (1999)
38. A.M. Arthurs, A. Dalgarno, Proc. R. Soc. A **256**, 540 (1960)
39. P. McGuire, D.J. Kouri, J. Chem. Phys. **60**, 2488 (1974)
40. R.T. Pack, J. Chem. Phys. **60**, 633 (1974)
41. R. Goldflam, D.J. Kouri, J. Chem. Phys. **66**, 542 (1977)
42. F. Thibault, B. Calil, J. Buldyreva, M. Chrysos, J.-M. Hartmann, J.-P. Bouanich, Phys. Chem. Chem. Phys. **3**, 3924 (2001)
43. T. Korona, R. Moszynski, F. Thibault, J.-M. Launay, B. Bussery-Honvault, J. Boissoles, P.E.S. Wormer, J. Chem. Phys. **115**, 3074 (2001)
44. F. Thibault, R.Z. Martinez, J.L. Domenech, D. Bermejo, J.-P. Bouanich, J. Chem. Phys. **117**, 2523 (2002)
45. T.G.A. Heijmen, R. Moszynski, P.E.S. Wormer, A. van der Avoird, A.D. Rudert, J.B. Halpern, J. Martin, W. Bin Gao, H. Zacharias, J. Chem. Phys. **111**, 2519 (1999)